

## TUNING THE MAGNETIC TRANSPORT OF AN INDUCTION LINAC USING EMITTANCE \*

T. Houck, C. Brown, M. Ong, A. Paul, P. Wargo, J. Zentler, LLNL, Livermore, CA 94550, U.S.A.

### Abstract

The Lawrence Livermore National Laboratory Flash X-Ray (FXR) machine is a linear induction accelerator used to produce a nominal 18 MeV, 3 kA, 65 ns pulse width electron beam for hydrodynamic radiographs. A common figure of merit for this type of radiographic machine is the x-ray dose divided by the spot area on the bremsstrahlung converter where a higher FOM is desired. Several characteristics of the beam affect the minimum attainable x-ray spot size. The most significant are emittance (chaotic transverse energy), chromatic aberration (energy variation), and beam motion (transverse instabilities and corkscrew motion). FXR is in the midst of a multi-year optimization project to reduce the spot size. This paper describes the effort to reduce beam emittance by adjusting the fields of the transport solenoids and position of the cathode. If the magnetic transport is not correct, the beam will be mismatched and undergo envelope oscillations increasing the emittance. We measure the divergence and radius of the beam in a drift section after the accelerator by imaging the optical transition radiation (OTR) and beam envelope on a foil. These measurements are used to determine an emittance. Relative changes in the emittance can be quickly estimated from the foil measurements allowing for an efficient, real-time study. Once an optimized transport field is determined, the final focus can be adjusted and the new x-ray spot measured. A description of the diagnostics and analysis is presented.

### INTRODUCTION

Time resolved emittance measurements using optical transition radiation have been performed in the past at FXR to characterize the beam quality [1]. The present effort is developing a methodology for using OTR measurements as a real time technique of tuning the beam transport focusing solenoids and other components to minimize emittance. Determining the absolute emittance from OTR for the relative low energy, high current beam of induction accelerators is challenging primarily due to radiation background. However, for tuning purposes, only the relative change in emittance is required. The issue now becomes how to discern which OTR pattern represents the lowest emittance. The next section explains possible sources of error and a methodology to minimize these errors. The paper finishes with a description of the experimental hardware and representative measurements.

\* This work was performed under the auspices of the U.S. Department of Energy by University of California, Lawrence Livermore National Laboratory under Contract W-7405-Eng-48.

### THEORY AND SIMULATIONS

OTR measurements determine the divergence or  $\sigma_{22}$  (see below) of the beam. If the radius and phase space tilt of the beam are known, the OTR information can be used to calculate the emittance. Experimentally, we attempt to perform OTR measurements under conditions where the beam has zero tilt, i.e. at a waist position. Errors due to non-waist conditions and an approach to minimizing these errors are described below.

#### *Effect of Non-waist Conditions*

Emittance can be expressed as:

$$\varepsilon = \sqrt{\sigma_{11}} \sqrt{\sigma_{22}} (1 - r_{12}^2)^{1/2}, \quad (1)$$

where  $r_{12} = \frac{\sigma_{12}}{\sqrt{\sigma_{11}\sigma_{22}}}$ , and  $\sigma_{11}$ ,  $\sigma_{22}$ , and  $\sigma_{12}$  are the sigma matrix elements [2] of the beam. Since emittance estimates from OTR measurements are usually assumed for waist conditions ( $r_{12} = 0$ ), the OTR and radius measurements yield  $\varepsilon_{OTR} = \sqrt{\sigma_{11}\sigma_{22}}$ . Thus, the effect of non-waist conditions at the OTR foil can be expressed in terms of a surprisingly simple equation:

$$\Delta\varepsilon_{rel} = \left( \frac{\varepsilon_{OTR} - \varepsilon}{\varepsilon} \right) = \left( \frac{1}{\sqrt{1 - r_{12}^2}} - 1 \right), \quad (2)$$

where  $\Delta\varepsilon_{rel}$  is the predicted error in the emittance estimate. Note that since  $r_{12}^2 \geq 0$ ,  $\Delta\varepsilon_{rel} \geq 0$ , the OTR emittance estimate should be a high estimate. Bear in mind, however, that the equation for  $\Delta\varepsilon_{rel}$  reflects only errors caused by off-waist conditions and does not include measurement errors and other possible sources of error.

Equation (2) performs well in simulations of a magnet scan, i.e. variations of a solenoid field, immediately upstream of the foil as indicated in Figure 1. Figure 1 compares the relative error from Equation (2) based on TRANSPORT [3] simulations and the error using emittance estimates from OTR Explorer [4] based on the TRANSPORT generated beam distribution, for magnet scans with two different transport tunes. The beam radius and  $r_{12}$  values are also plotted. The radius minimum does not exactly correspond to a waist condition in either scan, although the  $\Delta\varepsilon_{rel}$  values at these radius minima are small, 6% and 1%, respectively. Note, that it is possible to encounter higher  $\Delta\varepsilon_{rel}$  values at the radius minima for different scans. If more accurate waist locations are desired, and an accurate accelerator model is available, then simulations such as those used to generate Figure 1 can be used to predict the waist. However, in many cases, experimental determination of waist locations may be more appropriate, especially when determining model parameters for subsequent simulations.

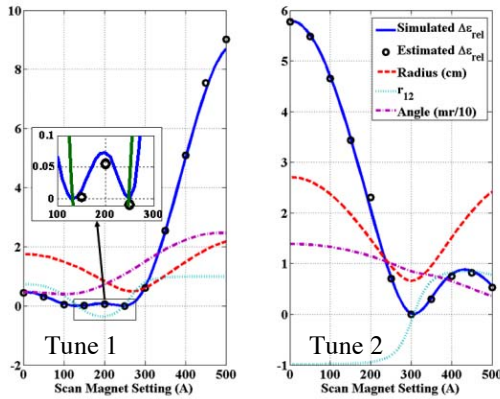


Figure 1: Comparison of Equation (2) with simulation.

### Experimentally Determining the Waist

We propose a simple algorithm for experimentally determining the locations of waists, or at least the minimum  $|r_{12}|$  points, which is based on both OTR and radius measurements. The algorithm consists of performing a magnet scan and estimating the emittance using the measured OTR and radius values and assuming waist conditions. The minima of the emittance values locate the minimum  $|r_{12}|$  points, and can be taken as accurate estimates of the beam emittance if  $r_{12} = 0$ . There is a tacit assumption that the scanned magnet is located near the foil and does not effect the beam emittance. Possible methods for establishing the existence of waists in a scan could be based on the shape of the predicted  $|r_{12}|$  curve that indicates a zero crossings.

Assuming there are waists in the scan, the relative difference between the estimated emittance for each scan setting and the minimum estimated emittance (the minimum of all the retrieved emittance values) can be used with Equation (2) to obtain  $|r_{12}|$ , which, using the radius and emittance estimates, can then determine  $\sigma_{22}$ . Thus, all sigma matrix parameters at the OTR foil (except for  $\sigma_{12}$ , the sign of which is not directly computed) can be derived from the OTR and radius data.

As an example, consider the simulated beam data used in Figure 1. The minima of the emittance values retrieved using OTR Explorer indicate the locations of the waists. If the emittance is taken to be the minimum of the retrieved emittance values, then the relative error in the emittance estimates is less than 1%. Converting the retrieved emittance values to the percentage difference relative to the minimum emittance value yields an estimate of  $|r_{12}|$ . The estimate of  $|r_{12}|$  and the simulated  $|r_{12}|$  are plotted in Figure 2.

Note that only TRANSPORT simulations have been used to simulate beam distribution to date. We hope to test the efficacy of the algorithm on real data in the future.

## HARDWARE

The hardware for acquiring the OTR/beam images is comprised of three major components: beam intercepting foil, optical packages, and cameras. The foil is viewed

with two separate camera/optical systems so that the OTR light pattern and beam profile are imaged simultaneously.

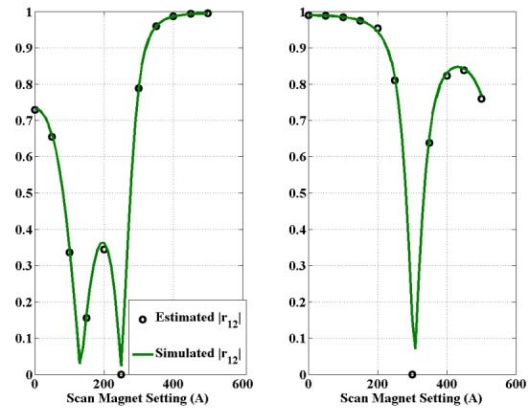


Figure 2: Demonstration of the algorithm for determining the waist using simulated data for the tunes in Figure 1.

### Foil

The beam is imaged on a 15 mil thick quartz foil with a 2,000 angstrom Al layer on the front and a fast scintillator phosphor (ZnO:Ga, 2 ns decay time) coating on the back. The OTR angular distribution was imaged from the aluminized side of the foil, while scintillation light is imaged from the phosphor side. The foil is mounted in a black anodized, aluminum holder attached to a manually operated linear inserter in a diagnostic cross at the downstream end of the FXR accelerator. In order to minimize scattered background light, the interior of the cross is anodized black. Proper orientation of the foil is verified by launching a HeNe alignment laser down the bore of the accelerator and adjusting the orientation of the foil such that the laser is reflected out of the diagnostic cross at 90 degrees to the beam axis.

### Optics

Two different optical lens systems are employed. The first system consists of a black Delrin cylinder housing a commercial Nikon 60 mm lens that focuses the beam image onto a fiber optic bundle attached at the rear of the cylinder. The entire assembly is held in place by an aluminum flange mounted directly to the diagnostic cross.

The second lens system is used to collect a suitable portion of the OTR angular pattern. The lens system was designed using the OSLO computer code to collect a full angle of at least  $4/\gamma$ , or about 7 degrees. We utilize a self-contained lens package consisting of a black anodized aluminum cylinder housing two 100 mm diameter achromatic lenses (e<sub>fl</sub> = 500 mm), a 80 mm diameter achromatic lens (e<sub>fl</sub> = 160 mm), a 50.8 mm diameter achromatic lens, and a custom 14.7 mm diameter SF11 lens (e<sub>fl</sub> = -12.8 mm) that project onto a fiber optic bundle attached at the rear of the cylinder. For viewing of the OTR angular pattern, the fiber optic bundle is located at the focal length of the lens package such that the system is focused at infinity; in this configuration, all rays of a given direction map to a single point regardless of

their spatial point of origin. The entire assembly is held in place by an aluminum flange mounted directly to the diagnostic cross such that the collection lenses are flush against the view port.

### Cameras

Two Princeton Instruments PI-MAX intensified CCD camera systems are used. Each camera is housed in an electromagnetically shielded box including approximately four inches of lead shielding. The cameras are triggered from a capacitively coupled probe on the output of one of the later stage MARX power units. The probe supplies a signal approximately 200 ns before the beam arrival to the Programmable Timing Generator (PTG). The cameras are stepped through the beam pulse in 5 to 10 ns steps to determine beam arrival time. The gate width is set to 2 ns.

## MEASUREMENTS

Sample images of the OTR light distribution and beam current distribution are shown in Figure 3. The images were taken approximately 20 ns into the energy “flat top” portion of the beam pulse. The background for the images is assumed to be primarily caused by Cherenkov and OTR from scattered electrons striking the view port glass. For the OTR light image background, we rotate the foil 20° such that the OTR light from the foil is outside the acceptance of the optics. The beam image background is taken from the image outside of the foil boundary.

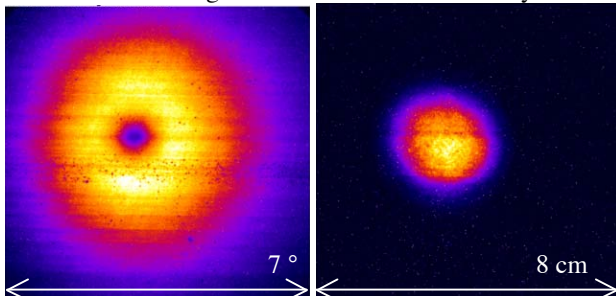


Figure 3: OTR light distribution and beam image in false colors. Backgrounds are subtracted and contrast ranges adjusted. Dark pixels/bands visible in the images are due to faults in the fiber optic bundle.

A tremendous amount of information can be discerned from these two images. The angular distance from the minimum of the OTR light to the maximum yields the beam energy ( $1/\gamma$ ). For this case, the energy was accurate to ~2%. The angular position of the light minimum within the image is a measure of the beam alignment with respect to the axis of the accelerator. Fitting the shape of the light distribution provides the divergence ( $\sqrt{\sigma_{22}}$ ). The beam image provides the current distribution and the radius ( $\sqrt{\sigma_{11}}$ ). The location of the current distribution within the image gives the beam centroid position with respect to the accelerator axis. Images for a scan of magnet values, including a waist, are needed to determine  $r_{12}$  and the beam emittance.

Measurements taken at different positions of the velvet cathode with respect to the shroud are shown in Figure 4. The nominal position (0.00) had about the lowest value for the radius times the OTR minimum to maximum (valley to peak or V/P) light ratio compared to moving the velvet in either direction. Emittance is approximately proportional to radius times the V/P ratio. The total beam current varied during the scan. To compensate for this effect, one set of measurements at maximum recess was taken at a higher diode voltage (57 kV Marx charge). This data yielded a significantly lower radius times V/P ratio. Further studies are planned.

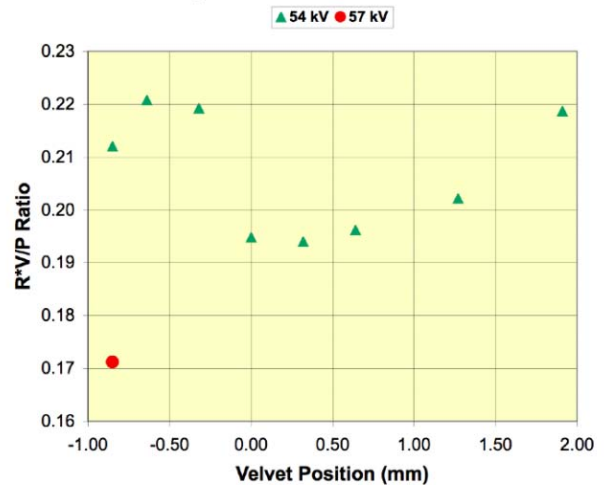


Figure 4: Variation in the relative emittance for various positions of the velvet with respect to the shroud.

## SUMMARY

Early attempts to adjust the transport of FXR to improve emittance was frustrated by the difficulty of determining when the emittance was actually improving. We now have a methodology for using OTR measurements at the exit of the accelerator to fully characterize the beam. By monitoring changes to these parameters as conditions in the accelerator are varied, we will be able to “tune” the accelerator for lower emittance.

## ACKNOWLEDGEMENTS

Nan Wong and Lynn Seppala designed the optics. Jim Dunlap, Blake Kreitzer, Keith Lewis, Al Traispe, and Sean Watson provided outstanding technical support.

## REFERENCES

- [1] J.S. Jacob, et al., “Time-resolved OTR Emittance Measurement,” LLNL, UCRL-TR-214037, (2005).
- [2] D. Carey, *The Optics of Charged Particle Beams*, (Harwood Academic Publishers, New York, 1987), pp. 99–122.
- [3] A.C. Paul, “Transport, an Ion Optic Program, LBL Version,” Lawrence Berkeley Lab LBL-2697 (1975).
- [4] OTR Explorer was written, and is distributed, by C. Ekdahl Los Alamos National Laboratory, NM.